Journal of Digital Imaging

Effect of Pixel Resolution on Texture Features of Breast Masses in Mammograms

Rangaraj M. Rangayyan,[1] Thanh M. Nguyen,[1] Fábio J. Ayres,[1] and Asoke K. Nandi[2]

The effect of pixel resolution on texture features computed using the gray-level co-occurrence matrix (GLCM) was analyzed in the task of discriminating mammographic breast lesions as benign masses or malignant tumors. Regions in mammograms related to 111 breast masses, including 65 benign masses and 46 malignant tumors, were analyzed at pixel sizes of 50, 100, 200, 400, 600, 800, and 1,000 μm. Classification experiments using each texture feature individually provided accuracy, in terms of the area under the receiver operating characteristics curve (AUC), of up to 0.72. Using the Bayesian classifier and the leave-one-out method, the AUC obtained was in the range 0.73 to 0.75 for the pixel resolutions of 200 to 800 μm, with 14 GLCM-based texture features using adaptive ribbons of pixels around the boundaries of the masses. Texture features computed using the ribbons resulted in higher classification accuracy than the same features computed using the corresponding regions within the mass boundaries. The *t* test was applied to AUC values obtained using 100 repetitions of random splitting of the texture features from the ribbons of masses into the training and testing sets. The texture features computed with the pixel size of 200 μm provided the highest average AUC with statistically highly significant differences as compared to all of the other pixel sizes tested, except 100 μm.

KEY WORDS: Breast cancer, breast masses, Haralick's texture features, mammography, margins of masses, pixel size, pixel resolution, ribbon around a mass, texture analysis, texture features, tumor classification, digital image processing, image analysis, mammography

INTRODUCTION

Texture analysis, using some or all of the 14 texture features proposed by Haralick et al.,[1] based upon gray-level co-occurrence matrices (GLCMs), is a popular approach for the analysis and classification of many medical images, including breast masses and tumors seen in mammograms.[2–4] Digital or digitized mammograms are usually acquired at the resolution of about 50 μm per pixel, with 4,096 gray levels represented using 12 bits per pixel (bpp). However, the GLCM of a 12-bpp image would be excessively large for practical computation; furthermore, most pairs of gray levels would occur with low or negligible rates of incidence that may not permit the derivation of reliable statistics. Therefore, in order to avoid sparse GLCMs, it is advantageous to reduce the image to 256 gray levels, that is, to use 8 bpp. A recent study by Lee et al.[5] compared the performance of texture features computed using 50, 100, and 400 levels of quantization of gray levels in the classification of breast masses; the highest level of classification accuracy was obtained with the combined use of the texture measures computed using all three levels of quantization. Our previous studies have shown that the GLCM-based texture features computed using a ribbon surrounding the region of interest (ROI) of a mass, also known as the margin of the mass, can lead to higher accuracy of discrimination between benign masses and malignant tumors, as

[1]*From the Department of Electrical and Computer Engineering, Schulich School of Engineering, University of Calgary, 2500 University Dr. NW, Calgary, Alberta, Canada T2N 1N4.*

[2]*From the Department of Electrical Engineering and Electronics, The University of Liverpool, Brownlow Hill, Liverpool, L69 3GJ, UK.*

This paper was submitted to the Journal of Digital Imaging, March 2009; revised July 2009.

Correspondence to: Rangaraj M. Rangayyan, Department of Electrical and Computer Engineering, Schulich School of Engineering, University of Calgary, 2500 University Dr. NW, Calgary, Alberta, Canada T2N 1N4; e-mail: ranga@ucalgary.ca

Online publication 12 September 2009
doi: 10.1007/s10278-009-9238-0

compared to the same texture features computed using the entire ROI.[6–8] The present study investigates the effect of pixel size or resolution on texture features, in terms of the accuracy of discrimination between benign masses and malignant tumors.

METHODS

Mammograms were obtained from the Mammographic Image Analysis Society (sampled at 50 μm per pixel), the teaching library of the Foothills Hospital in Calgary (sampled at 62 μm per pixel), and Screen Test: the Alberta Program for the Early Detection of Breast Cancer (sampled at 50 μm per pixel using the Lumiscan 85 scanner). Approval was obtained from the Conjoint Health Research Ethics Board, Office of Medical Bioethics, University of Calgary and Calgary Health Region, as well as from the Alberta Cancer Board. The images were quantized to 8 bpp, and have sizes of up to about 4,000×5,000 pixels. Regions in the mammograms related to 111 breast masses, including 65 benign masses and 46 malignant tumors, were identified and the contours of the masses were manually drawn by an expert radiologist specialized in screening mammography.[6–8] The sizes of the ROIs with benign masses vary in the range 32–1,207 mm^2, with an average of 214 mm^2 and a standard deviation of 206 mm^2. The sizes of the ROIs with malignant tumors vary in the range 34–1,244 mm^2, with an average of 277 mm^2 and a standard deviation of 285 mm^2. The diagnostic classification of the masses was based upon biopsy.

When mammographic films are sampled at about 50 μm per pixel, which is comparable to the resolution of the film, film-grain and other types of noise affect the quality of the image. Lowpass filtering and downsampling the images could reduce the effect of noise on the GLCM. Several studies have investigated the effect of using various pixel distances to compute the GLCM on the classification performance of GLCM-based texture features.[2,3] Using a pixel distance other than unity to compute the GLCM is equivalent to decimating the original image without applying an appropriate anti-aliasing filter to the image. In the present study, the downsampling procedure includes anti-aliasing filters. The criterion for the anti-aliasing filter for downsampling by a factor of 2, specified as a Gaussian, was a gain close to but less than 0.5 at one-half of the maximum frequency. This criterion resulted in the value of 0.75 for the standard deviation of the Gaussian, which was rounded up to 1.0 for a conservative filter design. The rounded value for the standard deviation of the Gaussian was scaled for other downsampling factors, as follows. The images were downsampled to effective pixel resolutions of 100, 200, 400, 600, 800, and 1,000 μm. The corresponding anti-aliasing Gaussian filters have standard deviation values of one, two, four, six, eight, and ten pixels. The filters were implemented using square mask (convolution matrix) sizes of seven, 13, 25, 37, 45, and 61 pixels, based upon the spatial extent of the non-negligible values in the corresponding Gaussian functions.

Ribbons of the masses were obtained by morphological dilation of the corresponding contours with a circular structuring element of diameter 160 pixels at the original resolution of 50 μm per pixel. The ROIs and ribbons of a benign mass and a malignant tumor are shown in Figure 1. The ribbon of a mass obtained in this manner includes parts at the periphery or margins of the mass inside and outside the boundary or contour provided; in this manner, the surrounding region of interaction of the mass with the neighboring elements is included in the analysis.

The GLCMs were computed at each level of pixel resolution, maintaining 256 levels of gray. Co-occurrences were combined for the four directions (0°, 45°, 90°, and 135°) with unit pixel distance at each level of resolution. All 14 texture features were computed for each ROI and ribbon at each level of resolution, using the definitions of Haralick et al.[1]; see Table 1 for the names and symbols used to represent the 14 features, and Haralick et al.[1] for details on the related methods.

In one of the options for pattern classification, the Bayesian classifier was employed.[9] The Bayesian classifier assumes that, for each class, the probability density function (PDF) of the feature vectors is a multivariate Gaussian function. As a consequence, the decision boundary is a quadratic function in the feature space. In another option for pattern classification, the Fisher linear discriminant (FLD) function,[9] which makes no assumption about the underlying PDF of the feature vectors

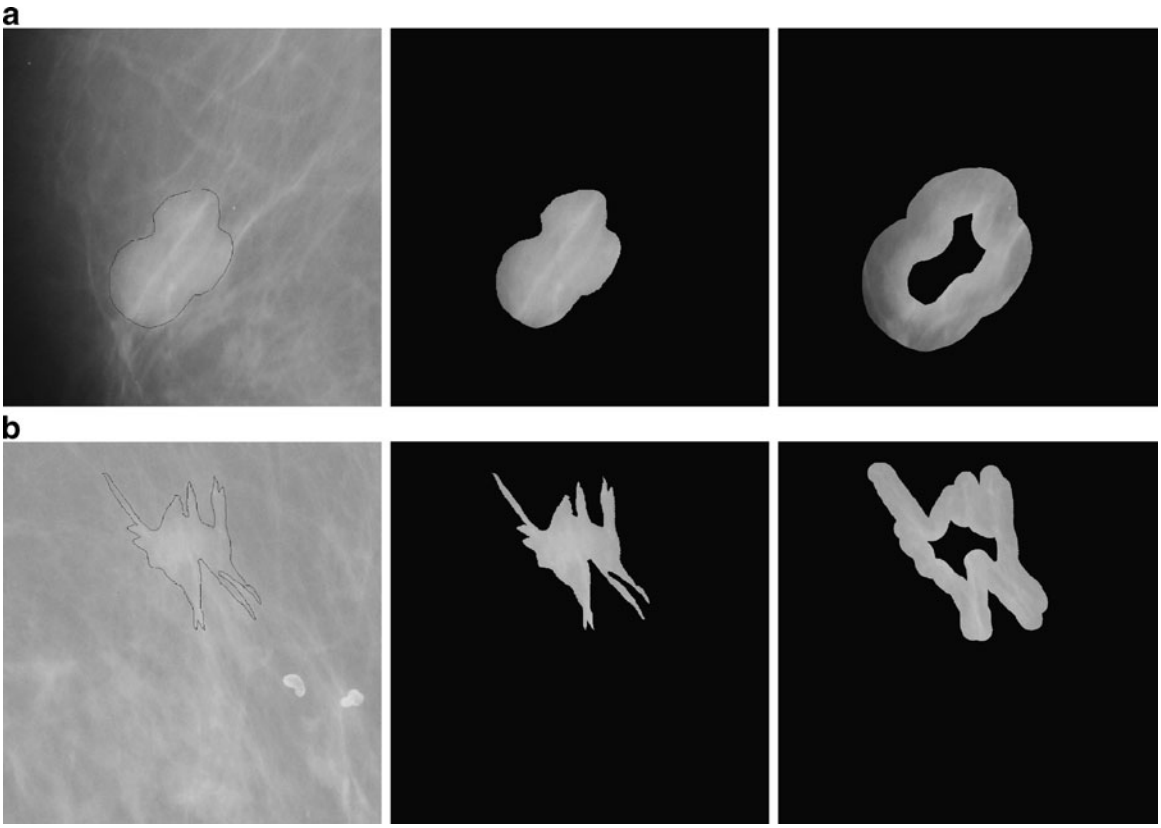

Fig 1. Examples of the contour, ROI, and ribbon of a a benign mass, and b a malignant tumor.

in each class, was used; the pooled sample covariance matrix of the two classes in the training set was used in formulating the classifier. The leave-one-out (LOO) procedure[9] was used to train and test the classifiers. The receiver operating characteristics (ROC) curve[10] was obtained for each experiment, and the area under the ROC curve (AUC) was derived to serve as a measure of the overall accuracy of the classifier and features. The discriminant capability of each feature was also assessed by deriving an ROC curve by applying a sliding threshold on the feature, and computing the related AUC value.

Based upon the results of the pattern classification experiments described above, the sets of 14 texture features computed from ribbons of masses at various pixel sizes were selected for further detailed evaluation using the Bayesian classifier and ROC analysis. The feature sets for the benign and malignant groups were randomly split so as to use 50% of the data in each group (benign or malignant) in the training phase of the classifier and to use the remaining 50% of the data in the testing phase. The random splitting procedure was applied 100 times and 100 values of AUC were obtained. In order the analyze the variability of AUC and the statistical significance of the differences between the results for the various pixel sizes considered, the mean and standard deviation values of the AUC values were obtained. The standard t test was applied to obtain the associated p values. (The LOO method provides a single AUC that is not amenable to the analysis of the variability of the accuracy of classification with different training and testing datasets.)

RESULTS

Table 1 lists the classification accuracy, in terms of AUC, for each individual texture feature computed from the ROIs and ribbons of the 111 masses tested, at the various pixel sizes considered. A sliding threshold was applied to each

feature to compute the measures required for ROC analysis; no trained classifier was used in this experiment. In classification experiments using each texture feature individually, the texture feature F_{10}, difference variance, gave the best classification results with a maximum AUC of 0.72, as well as high classification performance (AUC) across several levels of resolution. At certain levels of resolution, the texture features F_2, F_9, and F_{11} individually gave similar classification results, with AUC=0.72.

The results of pattern classification with FLD and LOO, listed in Table 2, indicate poor performance, with the maximal accuracy of AUC=0.71, achieved individually by F_9 and F_{11}, and by the combination of all 14 features computed using mass ribbons with pixel sizes of 800 and 1,000 μm. (Cases with the AUC under 0.5 are due to effects of the LOO procedure, and indicate that reliable separation between the two classes is not feasible under the circumstances of the associated experiments.) When the AUC values across all the FLD experiments were considered, the texture features F_1, F_4, and F_8 individually gave the best overall performance. The results indicate that benign masses and malignant tumors are not linearly separable, in the space defined by the 14 texture features, to a high level of classification accuracy.

The classification experiment using the Bayesian classifier and LOO (see Table 3) yielded higher values of AUC than FLD, with the best performance of AUC=0.75 given by the full set of 14 texture features computed using mass ribbons at the pixel resolutions of 400 and 800 μm. The values of AUC obtained using the texture features computed from the entire ROI and ribbons at several levels of pixel resolution with the Bayesian classifier are shown in Table 3. Individually, the feature F_{11} gave the best performance with AUC= 0.70; considering the AUC across all the experiments, the texture feature F_8 gave the most consistent performance. The results indicate that the use of a nonlinear classifier with all of Haralick's 14 texture features together, computed using ribbons of pixels around the masses, can provide higher performance in discriminating between benign masses and malignant tumors than the use of individual texture features and linear classifiers. It should be noted that, in cases with poor separation (or complete overlap) between the

Table 1. The Classification Accuracy, Measured in Terms of the AUC, for Haralick's Texture Features Computed from the ROI and Ribbons of 111 Masses at Several Levels of Pixel Resolution

		AUC												
Region	Pixel Resolution (μm)	Angular Second Moment (F_1)	Contrast (F_2)	Correlation (F_3)	Variance (F_4)	Inverse Difference Moment (F_5)	Sum Average (F_6)	Sum Variance (F_7)	Sum Entropy (F_8)	Entropy (F_9)	Difference Variance (F_{10})	Difference Entropy (F_{11})	Information Measure of Correlation (F_{12})	Information Measure of Correlation (F_{13})	Maximal Correlation Coefficient (F_{14})
ROI	50	0.63	0.54	0.68	0.70	0.51	0.51	0.70	0.70	0.64	0.54	0.53	0.65	0.69	0.67
	100	0.69	0.66	0.57	0.70	0.65	0.51	0.70	0.70	0.69	0.67	0.66	0.51	0.60	0.57
	200	0.71	0.71	0.51	0.70	0.70	0.50	0.70	0.70	*0.72*	0.71	0.71	0.58	0.54	0.51
	400	0.71	0.71	0.55	0.69	0.71	0.51	0.69	0.69	0.70	0.71	*0.72*	0.51	0.59	0.56
	600	0.68	*0.72*	0.55	0.69	0.70	0.51	0.69	0.67	0.66	0.71	*0.72*	0.61	0.65	0.53
	800	0.65	0.71	0.56	0.69	0.71	0.51	0.68	0.66	0.62	*0.72*	*0.72*	0.63	0.65	0.53
	1,000	0.60	*0.72*	0.56	0.69	0.70	0.51	0.68	0.63	0.57	*0.72*	0.71	0.63	0.64	0.51
Ribbon	50	0.59	0.51	0.65	0.64	0.54	0.58	0.64	0.66	0.59	0.53	0.52	0.64	0.68	0.65
	100	0.65	0.67	0.52	0.64	0.63	0.58	0.64	0.66	0.66	0.68	0.65	0.51	0.58	0.54
	200	0.69	0.71	0.56	0.64	0.68	0.58	0.64	0.66	0.69	*0.72*	0.69	0.59	0.51	0.53
	400	0.69	0.71	0.58	0.64	0.70	0.58	0.63	0.65	0.69	*0.72*	0.70	0.56	0.53	0.57
	600	0.68	0.70	0.58	0.63	0.70	0.58	0.62	0.64	0.67	0.70	0.70	0.52	0.58	0.57
	800	0.66	0.69	0.58	0.63	0.69	0.57	0.62	0.63	0.63	0.69	0.69	0.56	0.59	0.57
	1,000	0.62	0.68	0.58	0.63	0.69	0.57	0.61	0.61	0.60	0.68	0.69	0.56	0.58	0.56

A sliding threshold was applied to each feature; no trained classifier was used in this experiment
Instances of the highest AUC are shown in italics

Table 2. The Classification Accuracy, Measured in Terms of the AUC, for Haralick's Texture Features Computed from the ROI and Ribbons of 111 Masses at Several Levels of Pixel Resolution

		AUC														
Region	Pixel Resolution (μm)	All 14 Features	Angular Second Moment (F_1)	Contrast (F_2)	Correlation (F_3)	Variance (F_4)	Inverse Difference Moment (F_5)	Sum Average (F_6)	Sum Variance (F_7)	Sum Entropy (F_8)	Entropy (F_9)	Difference Variance (F_{10})	Difference Entropy (F_{11})	Information Measure of Correlation (F_{12})	Information Measure of Correlation (F_{13})	Maximal Correlation Coefficient (F_{14})
ROI	50	0.64	0.61	0.33	0.67	0.68	0.35	0.42	0.68	0.69	0.62	0.39	0.01	0.64	0.68	0.65
	100	0.63	0.67	0.61	0.54	0.68	0.63	0.41	0.68	0.69	0.68	0.62	0.64	0.01	0.57	0.54
	200	0.60	0.70	0.68	0.44	0.68	0.68	0.39	0.68	0.69	*0.71*	0.67	0.69	0.56	0.48	0.34
	400	0.61	0.70	0.68	0.52	0.68	0.70	0.31	0.67	0.67	0.69	0.69	0.70	0.36	0.56	0.52
	600	0.66	0.67	0.68	0.52	0.67	0.69	0.27	0.67	0.66	0.65	0.69	*0.71*	0.59	0.63	0.49
	800	0.59	0.64	0.69	0.54	0.67	0.70	0.24	0.66	0.64	0.61	0.69	*0.71*	0.61	0.63	0.48
	1,000	0.60	0.58	0.69	0.53	0.67	0.69	0.21	0.66	0.61	0.55	0.69	0.70	0.62	0.61	0.14
Ribbon	50	0.59	0.57	0.00	0.63	0.63	0.52	0.55	0.63	0.65	0.57	0.33	0.48	0.63	0.65	0.62
	100	0.66	0.64	0.61	0.43	0.63	0.62	0.55	0.63	0.65	0.64	0.63	0.63	0.38	0.54	0.46
	200	0.68	0.67	0.68	0.52	0.63	0.67	0.55	0.62	0.64	0.67	0.69	0.68	0.57	0.29	0.49
	400	0.68	0.68	0.68	0.55	0.62	0.68	0.55	0.61	0.64	0.68	0.69	0.69	0.54	0.44	0.54
	600	0.69	0.67	0.67	0.56	0.61	0.68	0.55	0.61	0.63	0.66	0.67	0.68	0.42	0.52	0.55
	800	*0.71*	0.64	0.66	0.55	0.61	0.68	0.55	0.60	0.62	0.62	0.66	0.68	0.53	0.52	0.55
	1,000	*0.71*	0.61	0.66	0.55	0.60	0.68	0.55	0.59	0.59	0.58	0.65	0.67	0.53	0.46	0.54

FLD analysis was used, with the LOO method for cross-validation
Instances of the highest AUC are shown in italics

Table 3. The Classification Accuracy, Measured in Terms of the AUC, for Haralick's Texture Features Computed from the ROI and Ribbons of 111 Masses at Several Levels of Pixel Resolution

		AUC														
Region	Pixel Resolution (μm)	All 14 Features	Angular Second Moment (F_1)	Contrast (F_2)	Correlation (F_3)	Variance (F_4)	Inverse Difference Moment (F_5)	Sum Average (F_6)	Sum Variance (F_7)	Sum Entropy (F_8)	Entropy (F_9)	Difference Variance (F_{10})	Difference Entropy (F_{11})	Information Measure of Correlation (F_{12})	Information Measure of Correlation (F_{13})	Maximal Correlation Coefficient (F_{14})
ROI	50	0.65	0.59	0.24	0.62	0.61	0.22	0.41	0.60	0.69	0.58	0.26	0.00	0.60	0.58	0.60
	100	0.65	0.62	0.45	0.40	0.59	0.62	0.42	0.59	0.69	0.67	0.43	0.63	0.00	0.42	0.41
	200	0.66	0.63	0.53	0.38	0.59	0.68	0.42	0.58	0.68	0.70	0.53	0.68	0.55	0.41	0.18
	400	0.69	0.62	0.55	0.51	0.57	0.70	0.43	0.56	0.67	0.69	0.54	0.70	0.23	0.47	0.44
	600	0.70	0.59	0.54	0.50	0.57	0.69	0.44	0.55	0.65	0.65	0.53	0.70	0.58	0.50	0.40
	800	0.67	0.53	0.58	0.55	0.56	0.69	0.43	0.53	0.64	0.60	0.58	0.70	0.61	0.53	0.36
	1,000	0.67	0.44	0.57	0.56	0.57	0.68	0.44	0.53	0.60	0.48	0.58	0.70	0.61	0.52	0.44
Ribbon	50	0.66	0.54	0.24	0.61	0.62	0.46	0.47	0.62	0.63	0.54	0.24	0.36	0.59	0.60	0.60
	100	0.71	0.61	0.46	0.26	0.62	0.59	0.47	0.62	0.63	0.62	0.45	0.60	0.28	0.45	0.32
	200	0.73	0.64	0.56	0.42	0.61	0.66	0.47	0.61	0.63	0.66	0.57	0.67	0.56	0.09	0.37
	400	*0.75*	0.65	0.55	0.49	0.60	0.68	0.47	0.60	0.62	0.67	0.56	0.68	0.51	0.32	0.48
	600	0.74	0.63	0.61	0.51	0.59	0.67	0.47	0.59	0.61	0.65	0.56	0.68	0.26	0.41	0.50
	800	*0.75*	0.55	0.62	0.54	0.59	0.67	0.46	0.58	0.60	0.61	0.60	0.67	0.45	0.41	0.54
	1,000	0.70	0.50	0.62	0.55	0.58	0.67	0.46	0.56	0.58	0.55	0.62	0.67	0.46	0.43	0.54

The Bayesian classifier was used, with the LOO method for cross-validation
Instances of the highest AUC are shown in italics

features of the two classes, use of the LOO method resulted in AUC values less than 0.5.

Table 4 lists the mean and standard deviation values of AUC obtained with 100 repetitions of 50% random splitting of the sets of 14 texture features into the training and testing parts of the Bayesian classifier. The ribbons of masses were used to compute the texture features. The highest mean AUC of 0.6464 was obtained at 200 μm per pixel. The results of the *t* tests indicated that the AUC values obtained at 200 μm per pixel are greater than those obtained at all other pixel sizes with high statistical significance ($p<0.01$), except 100 μm. The AUC values at 800 or 1,000 μm per pixel are lower than those at any other pixel size with high statistical significance ($p<0.01$); however, the AUC values at 800 μm vs those at 1,000 μm per pixel have no statistically significant difference. The AUC values for 50 μm per pixel are lower than those for 100 and 200 μm per pixel, and higher than those for 800 and 1,000 μm per pixel, with high statistical significance ($p<0.01$).

DISCUSSION AND CONCLUSION

Haralick's GLCM-based texture features have been used in several studies on medical images, including the studies by Sahiner et al.[11,12] and Mudigonda et al.[7] on mammographic masses. Although the features have provided good results in several applications, the classification performance obtained could vary significantly depending upon the nature of the images and the information contained therein. Our present study and a related preliminary study[13] indicate that the results are affected by several factors, including pixel resolution, preprocessing and filtering steps used, and the direction and distance used to compute the GLCMs.

The results of the present study indicate that ribbons or margins of masses at pixel resolution finer than 200 μm or coarser than 800 μm per pixel are unsuitable for use in the classification of mammographic masses, using all of the 14 texture features as defined by Haralick et al.[1] In the present study, the highest classification accuracy of AUC=0.75 was obtained by using ribbons of masses at the pixel sizes of 400 and 800 μm with the Bayesian classifier; however, comparable results were obtained at 200 and 600 μm per pixel (AUC=0.73 and 0.74, respectively). The use of coarse resolution (large pixel size) via downsampling of the original image could lead to the number of pixels available, in the case of small masses, being too low to permit the derivation of reliable GLCMs and texture features. In experiments with 100 repetitions of 50% random splitting of the data into the training and testing phases of the Bayesian classifier, the texture features computed with the pixel size of 200 μm provided the highest average AUC with statistically highly significant differences as compared to all of the other pixel sizes tested, except 100 μm. Based upon this result, we conclude that the pixel resolution of 200 μm is most suitable for the computation of GLCM-based texture features using ribbons or margins of masses.

The texture features computed using the ribbons of masses yielded higher classification accuracy than the same features computed using the entire mass ROIs. In this work, the width of each ribbon was fixed at 8 mm, regardless of the size of the mass. Mudigonda et al.[8] used a ribbon width proportional to the area of the mass; however, the numbers of pixels in such ribbons for small masses could become too low to permit the derivation of reliable GLCMs and texture features.

Several methods to perform feature selection were considered in preliminary work prior to the present study. However, feature selection methods

Table 4. Mean and Standard Deviation of the Classification Accuracy, Measured in Terms of the AUC, for Haralick's Texture Features Computed from the Ribbons of 111 Masses at Several Levels of Pixel Resolution

	Pixel resolution (μm)						
	50	100	200	400	600	800	1,000
Mean AUC	0.59	0.63	0.65	0.61	0.61	0.56	0.55
Standard deviation	0.07	0.06	0.07	0.07	0.08	0.07	0.07

The Bayesian classifier was used with 50% random splitting of the data into the training and testing parts for cross-validation, repeated 100 times. Please see the text for analysis of statistical significance of the differences in the results

could lead to different sets of features for the various cases of pixel size, mass ROIs, mass ribbons, and classifiers considered. Furthermore, the question arises as to whether features computed with different pixel sizes could be combined. For these reasons, no feature selection was performed in the present study so as to maintain the same set of 14 texture features for all subsequent experiments.

The present study has been limited to texture features; however, the work of Alto et al.[6] has shown that shape features can provide higher accuracy and complement texture features in classification, as well as content-based image retrieval; a study by Sahiner et al.[12] also leads to a similar observation. Recent classification experiments[14–16] with features of the same set of masses as in the present study with several nonlinear and kernel-based pattern classification methods, as well as feature selection and reduction of the dimensionality of features, have indicated the potential to achieve high levels of accuracy in discriminating between benign masses and malignant tumors. Further work with advanced classifiers could lead to higher classification accuracies than those reported in the present study. Further studies on the dimensions of the fibroglandular tissues in the breast that contribute to the appearance of texture in mammograms would be desirable.

The dataset used in the present study was prepared by combining digitized film mammographic images from three different sources. A similar study using direct digital mammographic images would be desirable. The images used in the study were not graded by breast density. Although the masses in the dataset used span the range from subtle to obvious, no ratings of subtlety were available. The effect of breast density and subtlety of masses on texture features needs to be studied.

The methods described in the present work could be used in conjunction with procedures for the detection and analysis of masses in mammograms for computer-aided diagnosis of breast cancer.

ACKNOWLEDGMENT

This project was funded by grants from the Canadian Breast Cancer Foundation: Prairies/NWT Chapter, the Alberta Heritage Foundation for Medical Research (AHFMR), the Natural Sciences and Engineering Research Council (NSERC) of Canada, and Research Services Office of the University of Calgary. This project was also supported by the Distinguished International Research Fellowship of the Schulich School of Engineering, University of Calgary, awarded to A. K. Nandi.

REFERENCES

1. Haralick RM, Shanmugam K, Dinstein I: Textural features for image classification. IEEE T Syst Man Cyb 3 (6):610–621, 1973

2. Sivaramakrishna R, Powel KA, Lieber ML, Chilcote WA, Shekhar R: Texture analysis of lesions in breast ultrasound images. Comput Med Imag Grap 26:303–307, 2002

3. Bovis K, Singh S: Detection of masses in mammograms using texture features. Proceedings of the 15th International Conference on Pattern Recognition; Sept 3–7, 2:267–270, 2000

4. Gupta S, Markey MK: Correspondence in texture features between two mammographic views. Med Phys 36(6):1598–1606, 2005

5. Lee GN, Hara T, Fujita H: Classifying masses as benign or malignant based on co-occurrence matrix textures: a comparison study of different gray level quantizations. In: Astley SM, et al Eds. International Workshop on Digital Mammography. Manchester, UK, LNCS 4046, 2006, pp 332–339

6. Alto H, Rangayyan RM, Desautels JEL: Content-based retrieval and analysis of mammographic masses. J Electron Imaging 14(2):023016, 2005, 1–17

7. Mudigonda NR, Rangayyan RM, Desautels JEL: Gradient and texture analysis for the classification of mammographic masses. IEEE T Med Imaging 19:1032–1043, 2000

8. Mudigonda NR, Rangayyan RM, Desautels JEL: Detection of breast masses in mammograms by density slicing and texture flow-field analysis. IEEE T Med Imaging 20:1215–1227, 2001

9. Duda RO, Hart PE, Stork DG: Pattern Classification, 2nd edition. New York: Wiley, 2001

10. Metz CE: Basic principles of ROC analysis. Semin Nucl Med 8:283–298, 1978

11. Sahiner BS, Chan HP, Petrick N, Helvie MA, Goodsitt MM: Computerized characterization of masses on mammograms: the rubber band straightening transform and texture analysis. Med Phys 25:516–526, 1998

12. Sahiner BS, Chan HP, Petrick N, Helvie MA, Hadjiiski LM: Improvement of mammographic mass characterization using spiculation measures and morphological features. Med Phys 28(7):1455–1465, 2001

13. Rangayyan RM, Nguyen TM, Ayres FJ, Nandi AK: Analysis of the effect of spatial resolution on texture features in the classification of breast masses in mammograms. Proc. Computer-assisted Radiology and Surgery, Berlin, Germany, June 2007. Springer, pp 334–336

14. Mu T, Nandi AK, Rangayyan RM: Classification of breast masses using selected shape, edge-sharpness, and texture features with linear and kernel-based classifiers. J Digital Imaging 21 (2):153–169, 2008

15. Mu T, Nandi AK, Rangayyan RM: Classification of breast masses via nonlinear transformation of features based on a kernel matrix. Med Biol Eng Comput 45(8):769–780, 2007

16. Nandi RJ, Nandi AK, Rangayyan RM, Scutt D: Classification of breast masses in mammograms using genetic programming and feature selection. Med Biol Eng Comput 44 (8):683–694, 2006